Abstract

Contents

1

Introduction

1.1 Quantum Computing

The idea of using a quantum mechanical system to simulate physics was first explored by Feynman[4]. Because the Hilbert space(/state space?) of a quantum mechanical system scales exponentially with it's size one would need an exponentially large classical computer to simulate it's behavior. By manipulating a quantum mechanical system directly this scaling problem can be circumvented.

It was quantum simulation that eventually led to the idea of exploiting quantum effects to perform more efficient calculations but it wasn't until Shor's discovery of a remarkably efficient quantum algorithm for prime factorization in 1994 [8] that quantum information science really took off.

Shor's algorithm was the first example where a quantum computer can provide an exponential speedup over a classical computer. Shor's and other quantum algorithms allow solving classes of previously impossible/unsolvable problems [remove?   such as the breaking of encryption].

Proof of principle experiments have been done in systems such as NMR [12]

By now Shor's algorithm has been shown to work on a range of different small scale quantum computers [12] [Needs reference to Shor in different systems or basic algorithms in range of systems] but making a scalable quantum computer that can take full advantage of the exponential speedup proves elusive.

1.2 Quantum Error Correction

1.3 Weakly coupled carbons; a naturally occurring register

2

Electronic spins in Diamond

Lorem ipsum dolor sit amet, consectetur adipisicing elit, sed do eiusmod tempor incididunt ut labore et dolore magna aliqua. Ut enim ad minim veniam, quis nostrud exercitation ullamco laboris nisi ut aliquip ex ea commodo consequat. Duis aute irure dolor in reprehenderit in voluptate velit esse cillum dolore eu fugiat nulla pariatur. Excepteur sint occaecat cupidatat non proident, sunt in culpa qui officia deserunt mollit anim id est laborum.

2.1 Spin Control

The Nitrogen Vacancy centre in diamond is a well investigated system [3] and a promising candidate for quantum computation [1]. In order to implement three qubit measurement based QEC we need three qubits plus ancillae that we can initialise, measure and conditionally perform operations on. These extra qubits are found in Carbon–13 atoms, which are normally a source of decoherence. These atoms can be addressed using a resonant decoupling sequence [9].

It has been shown that the nuclear- and electron- spin-state of the NV- centre can be initialized, coherently controlled and read-out using microwaves and laser pulses [7]. These are essential tools in controlling the NV- centre. In this chapter I will explain how control over the electron-spin-state can be used to address weakly coupled Carbon–13 atoms.

2.1.1 Spin Control

The electronic ground state Hamiltonian can be written as [6]:

$$H_{GS} = \Delta S_z{}^2 + \gamma_e \mathbf{B} \cdot \mathbf{S} \qquad (2.1)$$

With zero field splitting $\Delta \approx 2.88 \text{GHz}$ and gyromagnetic ratio $\gamma_e = 2.802 \text{ MHz/G}$. In this expression the interactions with the Nitrogen nucleus and the Carbon spin bath are not included. By applying a magnetic field B_z a long the N-V axis the degeneracy of the $m_s = \pm 1$ states is lifted by the Zeeman effect. A two level system that serves as a qubit can be defined with $m_s = 0 := |0\rangle$ and $m_s = -1 := |1\rangle$.

On the bloch-sphere the state vector rotates around the quantisation axis with a frequency depending on the energy splitting of the two states given by the Larmor frequency $\omega_L = \Delta - \gamma_e B_z$.[1] By applying an external field a term is effectively added to the Hamiltonian, changing the quantisation axis and thereby its evolution. By applying microwaves with the right frequency this can be used to selectively drive the transition from the $|0\rangle$ state to the $|1\rangle$state [5].

In a similar fashion the state of a Carbon–13 atom can be controlled by switching an additional term in the Hamiltonian on and off. The Hamiltonian of the nuclear spin depends on the electron state [11]:

$$H_0 = \gamma_C B_z I_z \qquad (2.2)$$

$$H_1 = \gamma_C B_z I_z + H_{HF} = \gamma_C B_z I_z + A_\parallel I_z + A_\perp I_x \qquad (2.3)$$

---

[1]When ω_L is used as a vector it is pointing in the $\hat{z}$ direction.

The the hyperfine term is not present when the electron is in the $m_s = 0$ state. The hyperfine term consists of a contact term and a dipole term. For carbons with weak couplings (A<200kHz) the contact term is expected to be negligible and the dipole term is given by [2]:

$$H_{dip} = \frac{\mu_0 \gamma_e \gamma_C \hbar^2}{4\pi r^3} [\mathbf{S} \cdot \mathbf{I} - 3(\mathbf{S} \cdot \hat{n}_{hf})(\mathbf{I} \cdot \hat{n}_{hf})] \tag{2.4}$$

From this equation the parallel and orthogonal components of the Hyperfine interaction, with respect to the N-V axis along the z direction, can be derived to be:

$$A_\parallel = -\frac{\mu_0 \gamma_e \gamma_C \hbar^2}{4\pi r^3} \left(3 \cdot \frac{z^2}{r^2} - 1 \right) \tag{2.5}$$

$$A_\perp = -\frac{\mu_0 \gamma_e \gamma_C \hbar^2}{4\pi r^3} \left(3 \cdot \frac{\sqrt{x^2 + y^2} \cdot z}{r^2} \right) \tag{2.6}$$
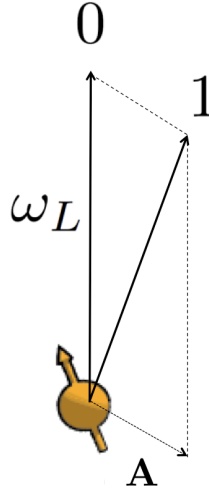

Figure 2.1 – Flipping the electron spin from the $m_s = 0$ to the $m_s = -1$ state changes the quantization axis of ^{13}C nuclear spins. For $m_s = 0$ spins precess about ω_L. For $m_s = -1$ spins precess about a distinct axis $\tilde{\omega} = \omega_\mathbf{L} + \mathbf{A}$ [10]

2.2   Structure of a typical experiment

Lorem ipsum dolor sit amet, consectetur adipisicing elit, sed do eiusmod tempor incididunt ut labore et dolore magna aliqua. Ut enim ad minim veniam, quis nostrud exercitation ullamco laboris nisi ut aliquip ex ea commodo consequat. Duis aute irure dolor in reprehenderit in voluptate velit esse cillum dolore eu fugiat nulla pariatur. Excepteur sint occaecat cupidatat non proident, sunt in culpa qui officia deserunt mollit anim id est laborum.

3
Weakly Coupled Carbon Spins

3.1 Addressing weakly coupled carbons trough dynamical decoupling

To understand how a Carbon–13 atom can be controlled it is useful to consider three situations. In the first situation ω_L and $\mathbf{A}$ point in the same direction. In the second situation ω_L and $\mathbf{A}$ are of comparable magnitude and point in different directions, resulting in a big angle between the quantisation axes. In the last situation A is small compared to ω_L resulting in a small angle between the quantisation axes.

When applying a decoupling sequence with N/2 decoupling units of the form $\tau - \pi - 2\tau - \pi - \tau$ the nuclear spin alternately rotates around the ω_L and the $\tilde{\omega}$ axis. The net result of one such decoupling sequence is a rotation around an axis $\hat{\mathbf{n}}_\mathbf{i}$ by an angle ϕ. Where $\hat{\mathbf{n}}_\mathbf{i}$ depends on the initial state of the electron [10].

When $\omega_\mathbf{L}$ and $\mathbf{A}$ point in the same direction, the net rotation axes are parallel making it impossible to control the Carbon–13 atom using this decoupling sequence.

In the case where ω_L and $\mathbf{A}$ are of comparable magnitude the net rotation axes $\hat{\mathbf{n}}_\mathbf{i}$ are strongly dependent on the initial state for almost any inter-pulse delay τ. Although this sounds nice as entanglement is almost always created, having two or more carbons with couplings comparable to the Larmor frequency creates complicated interactions.

When considering the case where $\mathbf{A}$ is small compared to ω_L the net rotation axes $\hat{n}_0$ and $\hat{n}_1$ are practically parallel and the nuclear spin undergoes an unconditional evolution. Only when the inter-pulse delay is precisely resonant with the spin dynamics the axes are antiparallel leading to a conditional rotation. The resonant condition occurs at [10]:

$$\tau = \frac{(2k+1)\pi}{2\gamma_C B_z + A_\parallel} \tag{3.1}$$

And for $\omega_L \gg \mathbf{A}$ the dip has a width of:

$$\Delta = \frac{A_\perp}{2 \cdot (\gamma_C B_z)^2} \tag{3.2}$$

If $\hat{n}_0$ and $\hat{n}_1$ are not parallel, the resulting conditional rotation of the nuclear spin generally entangles the electron and nuclear spins. As a result, for an unpolarised nuclear spin state, the final electron spin state is a statistical mixture of $|x\rangle$ and $|-x\rangle$ when starting from the $|x\rangle$ state. Where the probability that the initial state is preserved is given by:

$$P_x = (M+1)/2 \tag{3.3}$$

With for a single nuclear spin:

$$M = 1 - (1 - \hat{\mathbf{n}_0} \cdot \hat{\mathbf{n}_1}) \sin^2 \frac{N\phi}{2} \tag{3.4}$$

3.1.1 How many C13 can we control?

In reality the electron is not interacting with one carbon but with a bath of carbon atoms. When the electron interacts with multiple carbons at the same time M is given by the product of all individual values M_j for each individual spin j. In order to coherently control one carbon the electron should not entangle with any other carbon when addressing it.

In practice this means that the presence of a carbon that is strongly coupled (with respect to the Larmor frequency) makes it very hard to address any other carbon as entanglement is almost always created. It also means that resonances of weakly coupled (with respect to the Larmor frequency) carbons must not overlap. This excludes those carbons that are very weakly coupled in absolute terms as resonances of these carbons are located closely together.

As carbon–13 atoms are randomly distributed in the crystal the amount of weak resonances that can be addressed varies from NV to NV. By increasing the magnetic field the width and the delay-time of the resonances decreases. The downside is that it becomes harder to address these resonances as the resolution of the AWG used to apply the pulses is finite.

The question wether we can address enough carbon atoms to perform 3-qubit measurement-based quantum error correction was investigated using simulations and will be discussed in the next chapter.

3.2 Characterizing the Nuclear spin environment

Lorem ipsum dolor sit amet, consectetur adipisicing elit, sed do eiusmod tempor incididunt ut labore et dolore magna aliqua. Ut enim ad minim veniam, quis nostrud exercitation ullamco laboris nisi ut aliquip ex ea commodo consequat. Duis aute irure dolor in reprehenderit in voluptate velit esse cillum dolore eu fugiat nulla pariatur. Excepteur sint occaecat cupidatat non proident, sunt in culpa qui officia deserunt mollit anim id est laborum.
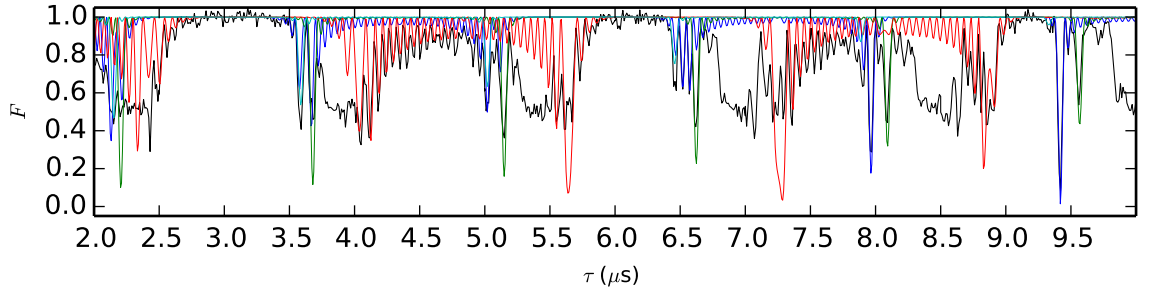

Figure 3.1 – Fingerprint of Hans Sil01 at B = 304.12G for N=32 pulses.

Carbon	$A_\parallel$	$A_\perp$
1	30.0 kHz·2π	80.0 kHz·2π
2	27.0 kHz·2π	28.5 kHz·2π
3	-51.0 kHz·2π	105.0 kHz·2π
4	45.1 kHz·2π	20.0 kHz·2π

Table 3.1 – Hyperfine paramters used to fit spins 1 to 4 in Figure 3.1.

Lorem ipsum dolor sit amet, consectetur adipisicing elit, sed do eiusmod tempor incididunt ut labore et dolore magna aliqua. Ut enim ad minim veniam, quis nostrud exercitation ullamco laboris nisi ut aliquip ex ea commodo consequat. Duis aute irure dolor in reprehenderit in voluptate velit esse cillum dolore eu fugiat nulla pariatur. Excepteur sint occaecat cupidatat non proident, sunt in culpa qui officia deserunt mollit anim id est laborum.

3.3 Controlling weakly coupled carbons trough the electronic spin

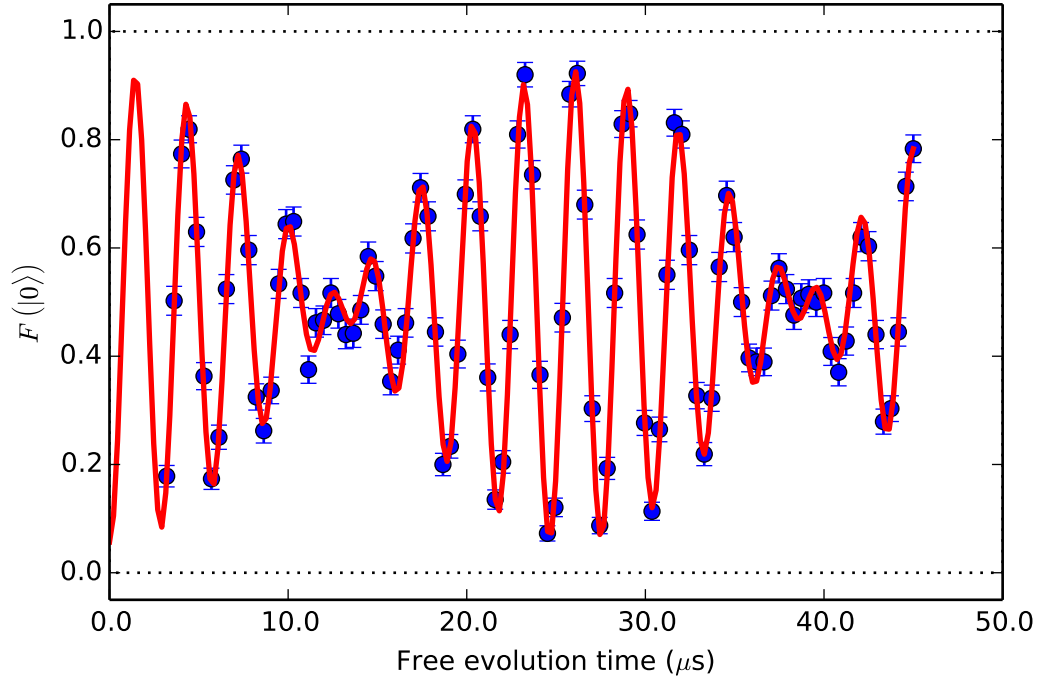## 3.4 Carbon Initialization & Readout
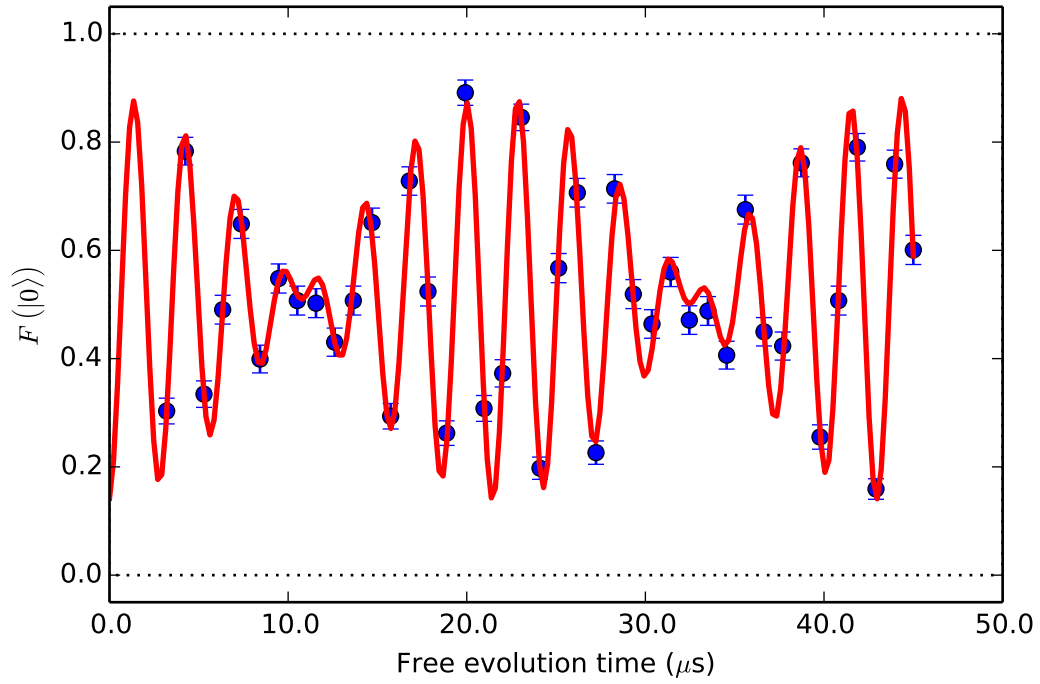
Figure 3.2 – Nuclear Ramsey of Carbon 1

Figure 3.3 – Nuclear Ramsey of Carbon 4

4

Deterministic Parity Measurements

4.1 Entanglement

4.2 Verification of Entanglement

5

Outlook: towards Quantum Error Correction

Lorem ipsum dolor sit amet, consectetur adipisicing elit, sed do eiusmod tempor incididunt ut labore et dolore magna aliqua. Ut enim ad minim veniam, quis nostrud exercitation ullamco laboris nisi ut aliquip ex ea commodo consequat. Duis aute irure dolor in reprehenderit in voluptate velit esse cillum dolore eu fugiat nulla pariatur. Excepteur sint occaecat cupidatat non proident, sunt in culpa qui officia deserunt mollit anim id est laborum.

Bibliography

[1] L. Childress and R. Hanson. Diamond nv centers for quantum computing and quantum networks. *MRS Bulletin*, 38(02):134–138, 2 2013.

[2] G. de Lange. *Quantum Control and Coherence of Interacting Spins in Diamond*. PhD thesis, Delft University of Technology, 2012.

[3] M.W. Doherty, N.B. Manson, P. Delaney, F. Jelezko, J. Wrachtrup, and L.C.L. Hollenberg. The nitrogen-vacancy colour centre in diamond. page 101, 2 2013.

[4] Richard P. Feynman. Simulating physics with computers. *International Journal of Theoretical Physics*, 21(6-7):467–488, 6 1982.

[5] F. Jelezko, T. Gaebel, I. Popa, a. Gruber, and J. Wrachtrup. Observation of coherent oscillations in a single electron spin. *Physical Review Letters*, 92(7):076401, 2 2004.

[6] W. Pfaff. *Quantum Measurement and Entanglement of Spin Quantum Bits in Diamond*. PhD thesis, Delft University of Technology, 2013.

[7] L. Robledo, L. Childress, H. Bernien, B. Hensen, P.F.A. Alkemade, and R. Hanson. High-fidelity projective read-out of a solid-state spin quantum register. *Nature*, 477(7366):574–8, 9 2011.

[8] P.W. Shor. Algorithms for quantum computation: discrete logarithms and factoring. In *Proceedings 35th Annual Symposium on Foundations of Computer Science*, pages 124–134. IEEE Comput. Soc. Press, 1994.

[9] T. H. Taminiau, J. J. T. Wagenaar, T. van der Sar, F. Jelezko, V. V. Dobrovitski, and R. Hanson. Detection and control of individual nuclear spins using a weakly coupled electron spin. *Physical Review Letters*, 109(13):137602, 9 2012.

[10] T. H. Taminiau, J.J.T. J. T. Wagenaar, T. van der Sar, F. Jelezko, V.V. V. Dobrovitski, and R. Hanson. Detection and control of individual nuclear spins using a weakly coupled electron spin. *Physical Review Letters*, 109(13):137602, 9 2012.

[11] T. H. TH Taminiau, J. Cramer, T. van der Sar, V. V. Dobrovitski, and R. Hanson. Universal control and error correction in multi-qubit spin registers in diamond. *Nature Nanotechnology*, 2(February):2–7, 9 2014.

[12] L M Vandersypen, Matthias Steffen, Gregory Breyta, Costantino S Yannoni, Mark H Sherwood, and Isaac L Chuang. Experimental realization of shor's quantum factoring algorithm using nuclear magnetic resonance. *Nature*, 414(6866):883–7, 2001.

A

State Initialization

B

Bell State Tomography

Derivation, what would a tomography of the Psi+ state look like?

C

Entanglement wittness

D

Simulations

Acknowledgements